# Modeling of electronic properties of electrostatic quantum dots

S. Bednarek, B. Szafran, K. Lis, and J. Adamowski*
*Faculty of Physics and Nuclear Techniques, AGH University of Science and Technology, al. Mickiewicza 30, 30-059 Kraków, Poland*
(Received 7 July 2003; published 29 October 2003)

Electrostatic (gated) quantum dots are studied by computational methods. Electronic properties of the electrostatic quantum dots are determined by the confinement potential, which is created by external voltages, applied to the electrodes, and band offsets. We have solved the Poisson equation for the two-terminal quantum dot nanodevice made of several GaAs and AlGaAs layers and obtained the confinement potential profile in the entire nanodevice. We show how the confinement potential profile can be modeled, which allows us to design—to some extent—the required electronic properties of the nanodevice. The results have been confirmed by a good agreement with experimental data. We have discussed the similarities and differences between the two- and three-terminal quantum dot nanodevices studied experimentally by Ashoori *et al.* [Phys. Rev Lett. **71**, 613 (1993)] and Tarucha *et al.* [Phys. Rev. Lett. **77**, 3613 (1996)], respectively.

DOI: 10.1103/PhysRevB.68.155333 PACS number(s): 73.21.La

## I. INTRODUCTION

Electrons localized in a quantum dot (QD) by a confinement potential occupy atomiclike states with discrete energy levels. Therefore, the QD with the confined electrons is called the artificial atom.[1] In the electrostatic (gated) QD's,[2–5] which are studied in the present paper, the confinement potential results from the external voltages, applied to the electrodes, and band offsets. The confinement potential is very sensitive to the voltages applied as well as the parameters of the nanostructure, in particular, the geometry of the nanodevice and doping. The electronic properties of the nanodevice are determined by the confinement potential. Therefore, the knowledge of the realistic profile of this potential is important for a design of the nanodevice with the required electronic properties and for a theoretical description of the confined electron states.

A direct experimental determination of the confinement potential is not possible. Therefore, the confinement potentials used in the majority of theoretical papers possess the model character.[1,6–12] The model parabolic potential and rectangular potential well are the most common of them. Moreover, the Gaussian[11] and power-exponential[12] confinement potentials were also applied. These models usually neglect the dependence of the confinement potential on the voltages applied to the electrodes and number $N$ of electrons confined in the QD. The model parabolic potential with the confinement frequency dependent on $N$ was also applied to the QD's.[13–15] If the realistic profile of the confinement potential is unknown, an unambiguous interpretation of the experimental data is difficult or even impossible. The shape of the confinement potential can be calculated by suitable theoretical approaches.[16–21] In self-assembled QD's, the confinement potential, which depends on the band offsets and the strain between the QD and substrate materials, can be calculated in the framework of the elasticity theory.[18] In electrostatic QD's, the confinement potential generated by the external voltages applied to the leads can be calculated from the Poisson equation.[16,17,19–21] In Refs. 20 and 21, a self-consistent procedure was elaborated for the solution of the Poisson-Schrödinger problem in the three-electrode vertical QD of Tarucha et al.[5] The calculated[20,21] realistic profile of the confinement potential takes into account the voltages applied to the leads, the spatial distribution of the ionized donors, and the electrons confined in the QD. The results of calculations[20,21] very well agree with the experimental data.[5,22]

Both types of electrostatic QD's, i.e., the first one made by Ashoori *et al.*[3] and the second one made by Tarucha et al.[5], are still intensively studied experimentally.[23–25] Recently, in the two-electrode QD[3] the localization-delocalization transition has been found,[23] and in the three-electrode QD[5] the Kondo effect has been observed.[25]

In our recent paper,[26] we have considered the two-electrode QD, which was fabricated on the basis of the planar nanostructure by Ashoori *et al.*[2–4,27] We have shown[26] that the confinement potential can take on different shapes: from a flat-bottom and steep-wall potential, which can be approximated by the rectangular potential well, to the smooth potential, which can be approximated by either a Gaussian or a parabolic potential.

In the present paper we extend this research[26] and perform a detailed study of the effects of the geometric structure and doping on the profile of the confinement potential. Taking into account the charges induced on the leads, we can determine the dependence of the confinement potentials on the gate voltage and the number of electrons confined in the QD. We have verified the quality of the calculations by applying them to a description of the capacitance spectroscopy data.[3] Having at disposal a computational tool for determining the realistic confinement potentials, we have performed an optimization of the nanodevice parameters and studied the sensitivity of the confinement potentials to the changes of these parameters.

The paper is organized as follows: in Sec. II we present the theoretical approach and check its reliability, and in Sec. III we provide the results of the optimization of the nanodevice parameters. Section IV contains the discussion and Sec. V the conclusions.

## II. THEORY

### A. Model nanodevice

A schematic of the nanodevice considered in the present paper is pictured in the inset of Fig. 1. The present model

 

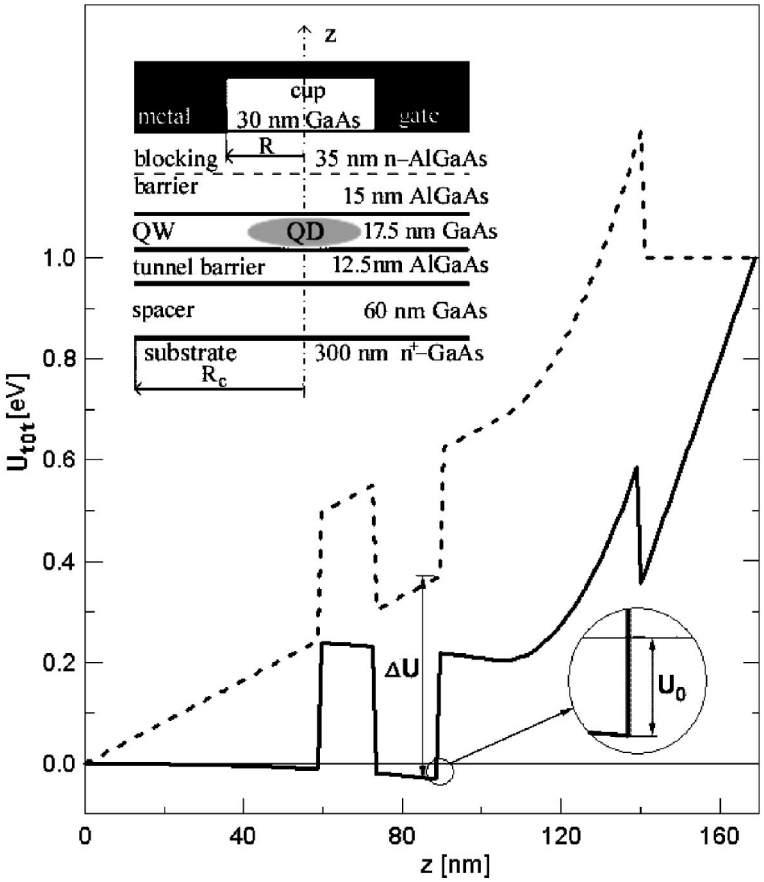


FIG. 1. Boundary conditions put on total potential energy $U_{tot}$ for $r=R_c$ (dashed curve) and $U_{tot}$ along the cylinder axis (solid curve) as functions of $z$. $U_0$ and $\Delta U$ are the vertical and lateral confinement potential depths, respectively. Thin horizontal line corresponds to the Fermi energy. Inset: Schematic of the nanodevice used in the calculations.

approximates quite well the real QD's studied by Ashoori *et al.*[2–4,27] The nanodevice[2,3] has a planar structure and consists of the doped and undoped GaAs and AlGaAs layers. The 300-nm-thick GaAs substrate layer is heavily doped by donors and forms the bottom electrode. The subsequent layers, grown on the substrate, form the following sequence: the 60-nm GaAs spacer, the 12.5-nm AlGaAs tunnel barrier, the 17.5-nm GaAs quantum well, and the 50-nm AlGaAs blocking barrier, in which the lower 15-nm sublayer is undoped and the upper 35-nm sublayer is doped by donors. In the nanostructures[3,4,27] a $\delta$ doping of the blocking barrier was applied. In the present calculations, we take this doping into account by smearing the charge of the ionized donors over the entire upper 35-nm AlGaAs barrier sublayer. The 30-nm GaAs cylindrical cap of radius $R$ is grown on the $n$-doped AlGaAs barrier layer. The entire structure is covered with the metal layer, which forms the top gate. The voltage applied between the gate and bottom electrode is a source of the inhomogeneous electrostatic field, which—in the region below the cap—generates the potential confining the electrons laterally within the GaAs quantum well. The vertical confinement results from the GaAs/AlGaAs conduction-band offsets. The physical region of the QD is located within the GaAs quantum-well layer below the cap. For the fixed thicknesses and compositions of the layers the radius of the cap determines the shape of the confinement potential.

### B. Poisson equation

The total electrostatic field that confines electrons in the QD is generated by the external potential applied to the gate, the ionized donor centers in the $n$-doped layers, and the electrons confined in the QD. In order to take into account the dependence of the confinement potential on the confined charge carriers, we apply the superposition principle and separate[21] potential $\Phi$ of the total electrostatic field into two components, which stem from different sources, i.e.,

$$\Phi(\mathbf{r})=\varphi_1(\mathbf{r})+\varphi_2(\mathbf{r}), \tag{1}$$

where $\varphi_1$ is the potential of the electrostatic field, which is generated by the charges of the ionized impurities and the charges on the leads, and $\varphi_2$ is the potential of the electrostatic field created by the electrons confined in the QD. Potential $\varphi_2$ is identified with the Hartree potential.[21] Potential $\varphi_1$ is found by solving the Poisson equation

$$\nabla^2\varphi_1(\mathbf{r})=-\frac{\varrho(\mathbf{r})}{\varepsilon\varepsilon_0}, \tag{2}$$

where $\varrho(\mathbf{r})$ is the density of the charge associated with the ionized donors in the AlGaAs blocking barrier layer and in the thin interface layer of the GaAs substrate. In the present calculations, we take on the static dielectric constant $\varepsilon$ for GaAs. When solving Eq. (2), we impose the boundary conditions on total potential $\Phi$ and calculate the boundary values of $\varphi_1$ from Eq. (1). This procedure, described in detail in Ref. 21, allows us to include the charges induced in the leads by the electrons confined within the QD.

The boundary conditions are put on the cylindrical surface with radius $R_c$, which encompasses the integration domain

(cf. inset of Fig. 1). The inner surfaces of the top gate and bottom electrodes are taken as the cylinder bases. The potentials on these electrodes are set in experiments[2–4] and therefore are known. The boundary conditions on the cylindrical side surface are determined as follows: we assume that radius $R_c$ of the cylinder is so large that the electric field on this surface is approximately parallel to the cylinder axis. Next, we take the potential profile on this boundary surface according to Fig. 1. In the nanostructure considered, Poisson equation (2) possesses the full cylindrical symmetry and is reduced to

$$\left(\frac{\partial^2}{\partial r^2}+\frac{1}{r}\frac{\partial}{\partial r}+\frac{\partial^2}{\partial z^2}\right)\varphi_1(r,z)=-\frac{\varrho(r,z)}{\varepsilon\varepsilon_0}. \qquad (3)$$

We solve Eq. (3) by the finite-difference relaxation method on the two-dimensional mesh.[21] Figure 1 also displays the potential energy calculated along the cylinder axis. This potential takes into account the band offsets and the Schottky barrier, which act as additional fields in the vertical ($z$) direction.

### C. Reliability of the model

In the calculations, we have taken the Schottky barrier between the gate and GaAs semiconducting layer to be 0.65 eV (Ref. 28) and the shift of the conduction-band bottom of GaAs with respect to that of AlGaAs equal to 220 meV. In order to check the present model we have applied it to a quantitative description of the capacitance-spectroscopy data.[3] The spectrum of electrons confined in the QD is additionally affected by a fluctuating potential, which stems from randomly distributed impurities and surface defects. In the present model we neglect this fluctuating potential. Therefore, for the test calculations we have chosen the QD (Ref. 3) with the possibly small radius, for which the effect of the fluctuating potential is the smallest.

Among several parameters of the nanostructure, two of them cannot be determined in experiments with the sufficient precision. These are radius $R$ of the cap, which cannot be accurately measured because of the undercut of the GaAs cap due to the etching,[21] and concentration $n_D$ of the ionized Si donors in the blocking barrier, since during the intentional doping not all Si atoms occupy the donor sites in AlGaAs and moreover not all the donors are ionized.[29] The radius of the cap determines the profile of the confinement potential, which in turn affects the energy separations between the capacitance-spectroscopy peaks, while the concentration of the ionized donors determines the gate voltage, for which the first electron becomes trapped in the QD. We have adjusted the values of $R$ and $n_D$ in order to reproduce the capacitance peaks,[3] which correspond to the closed shells of the artificial atom.

Let us note that—in the absence of external fields and at zero temperature—Fermi energy $E_F$ of the entire nanodevice is determined by the ground-state energy of the donors in the substrate. Throughout the present paper, we take the Fermi energy as the reference energy and put $E_F=0$.

Figure 2 shows the chemical potential calculated as $\mu_N$

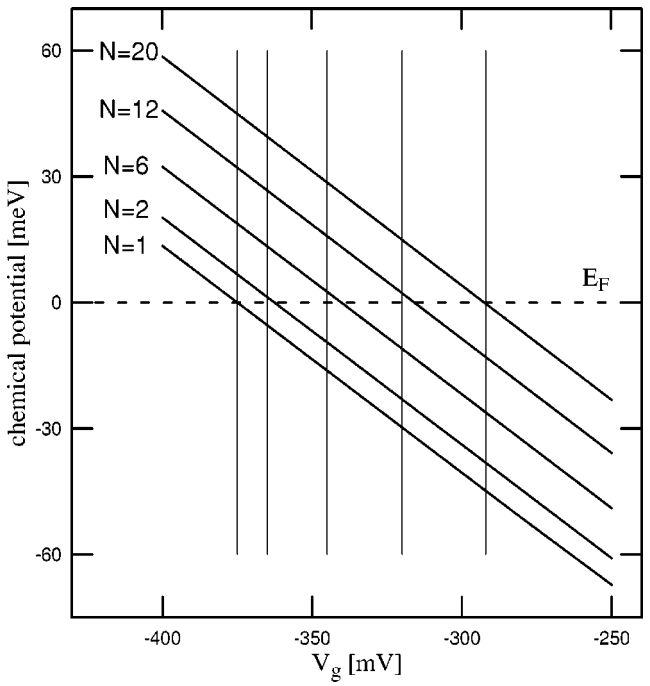


FIG. 2. Chemical potential $\mu_N$ as a function of gate voltage $V_g$ for several numbers $N$ of electrons confined in the QD. Dashed horizontal line displays Fermi energy $E_F$ and thin vertical lines show the positions of the capacitance spectroscopy peaks from Ref. 3.

$=E_N-E_{N-1}$, where $E_N$ is the ground-state energy of $N$ electrons confined in the QD. In the present paper, energy $E_N$ has been calculated by the Hartree-Fock method. The results for the artificial atoms with $N=1$, 2, 6, 12, and 20 electrons, for which the electronic shells of the cylindrically symmetric artificial atom are closed, are compared with the measured positions of the capacitance-spectroscopy peaks.[3] We determine the positions of the capacitance peaks from the crossing points of the chemical potential of $N$ electrons confined in the QD with the Fermi energy.[21] Figure 2 shows that adjusting only two parameters we have accurately reproduced the positions of six capacitance peaks. The largest deviation of 5 mV occurs for $N=6$. The results of Fig. 2 have been obtained with $R=205$ nm and $n_D=4.62\times10^{17}$ cm$^{-3}$, which corresponds to the two-dimensional ionized donor concentration $1.6\times10^{12}$ cm$^{-2}$ in the $\delta$-doped layer.

Using the fixed values of both adjusted parameters we have checked the reliability of the present model by calculating the magnetic-field dependence of the first two capacitance peaks.[3] In this case, we deal with the one- and two-electron systems, for which the energy levels can be calculated with the arbitrary accuracy by the imaginary-time method.[30] These results are free of the correlation errors, which shift the critical magnetic fields for the phase transitions.[31] Therefore, they can be treated as ''exact.'' Solid curves in Fig. 3 display the chemical potential, which corresponds to the single-electron charging of the QD. We see that the agreement with the experimental data[3] is good. In particular, the present calculations very well reproduce the position of the kink, which results from the singlet-triplet tran-

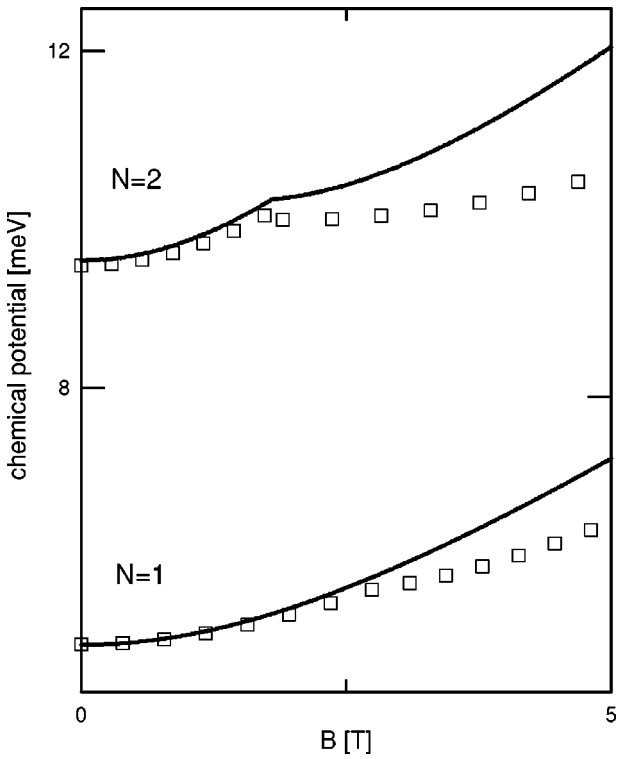


FIG. 3. Chemical potential calculated (solid curves) for $N=1$ and $N=2$ electrons as a function of magnetic field $B$. The experimental data (Ref. 3) are marked by squares.

sition in the two-electron QD-confined system.[32,33] This agreement means that the shape of the potential (oscillator energy) is correctly calculated from the Poisson equation. We note that fitting the confinement energy to the magnetic-field dependence of the one-electron ground state leads to $\hbar\omega_0 = 5.4$ meV,[3] which in turn yields the position of the singlet-triplet crossing overestimated by a factor of 2. We remark that the curves calculated in the present paper slightly deviate from the experimental plots at high magnetic fields, which can result from neglecting some additional effects, e.g., we cannot exclude a small shift of the Schottky barrier in the magnetic field.

## III. RESULTS

### A. Confinement potential profile

Figure 4 shows the total potential energy of the electron calculated for the nanodevice of Ashoori *et al.*[3] Total potential energy $U_{tot}$ of the electron is the sum of the band offsets and the electrostatic confinement potential energy $U$, which is defined as

$$U(r,z) = -e\varphi_1(r,z), \tag{4}$$

where $e>0$ is the elementary charge. The position of the Fermi energy is marked by the thick solid line. In the nanodevice,[3,27] the electrons can occupy the QD region in the quantum-well layer and also a part of GaAs spacer close to the barrier layer (cf. Fig. 4). In the present paper, we consider only the electrons confined in the quantum well.

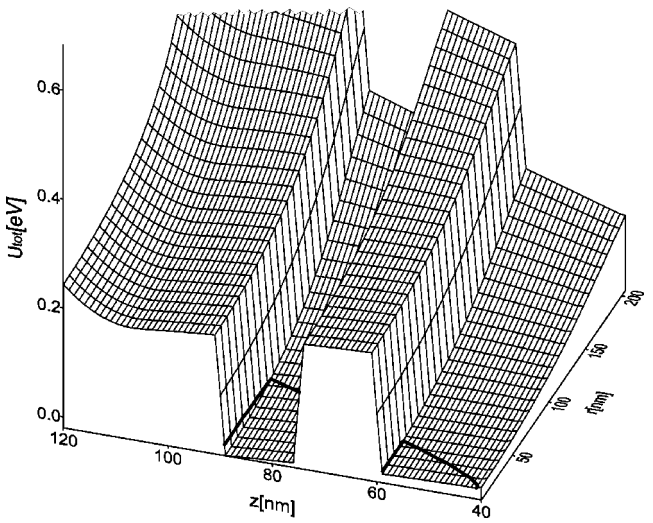


FIG. 4. Total potential energy $U_{tot}$ of the electron in the nanodevice as a function of cylindrical coordinates $r$ and $z$. Thick solid line corresponds to the Fermi energy.

Figure 5 displays the electrostatic lateral confinement potential energy, defined as $U(r,z_0)$ for $z_0$ fixed within the QD region. The thick solid line corresponds to the Fermi energy, which is shifted by the one-electron ground-state energy of the quantized motion in the $z$ direction. Figure 5 shows that the lateral confinement potential energy can be approximated by a parabolic function of $r$. Figure 5 also shows the effect of the charge confined in the QD. The increasing (negative)

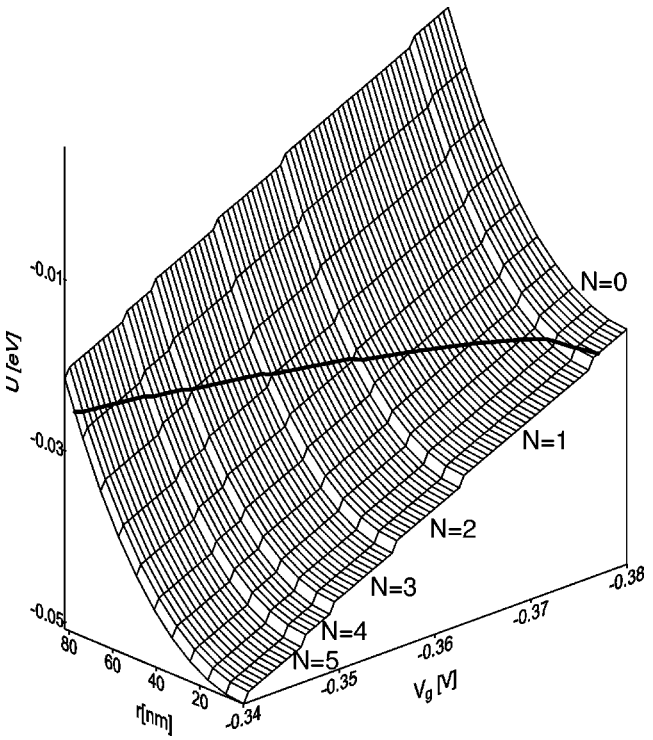


FIG. 5. Electron confinement potential energy $U$ as a function of lateral distance $r$ and gate voltage $V_g$. Thick solid line corresponds to the Fermi energy. The energy is measured with respect to the one-electron ground-state energy of the vertical quantized motion.

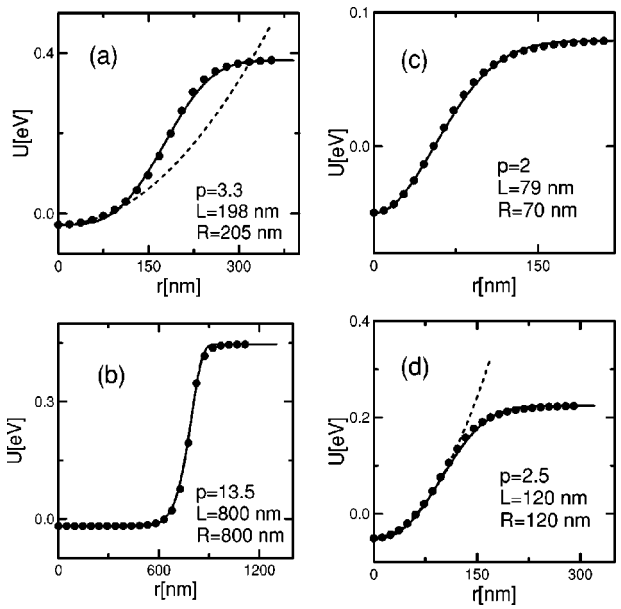


FIG. 6. Lateral confinement potential energy $U(r,z_0)$ as a function of $r$. Dots show the numerical solutions of Poisson equation (3), solid curves show fitted power-exponential function (5), and dashed curves show fitted parabolic function. The results for (a) the QD with parameters compatible with those of Ref. 2 and 3, (b) flat-bottom, steep-wall potential well, (c) Gaussian potential well, and (d) parabolic potential well over a large part of the QD. Cap radius $R$ and fitted parameters, i.e., power $p$ and range $L$, of power-exponential potential (5) are quoted.

gate voltage lowers the electron potential energy. This leads to the localization of the subsequent electrons in the QD, which in turn results in a further stepwise lowering of the confinement potential energy. Figure 5 shows the modification of the confinement potential by the electrons confined in the QD. This effect is caused by the charge induced on the leads. A similar stepwise dependence on the number of QD-confined electrons has been found[21] in the three-electrode vertical QD.[5] However, contrary to the three-terminal QD nanodevice,[21] the shape of the lateral confinement potential in the two-terminal QD nanodevice remains unchanged when changing the gate voltage.

We have applied the present approach to a modeling of the confinement potential profile. For this aim we study the QD considered in Sec. II, but we now vary cap radius $R$ and gate voltage $V_g$. The shape of the confinement potential is very sensitive to the cap radius, while the gate voltage is mainly responsible for the position of the potential-well bottom. Therefore, changing $R$ we can model the confinement potentials with different profiles. The results are shown in Figs. 6(a)–6(d). In each case, the value of gate voltage $V_g$ has been chosen so that exactly one electron is bound in the QD. Figures 6(a)–6(d) show the lateral confinement potential energy $U(r,z_0)=-e\varphi_1(r,z_0)$, calculated from Poisson equation (3), where $z_0$ is taken within the quantum-well layer. Figures 6(a)–6(d) also display the power-exponential model confinement potential energy,[12] i.e.,

$$U(r)=-U_0\exp[-(r/L)^p], \tag{5}$$

which has been fitted to the numerical solutions of the Poisson equation. Parameter $L$ determines the lateral range of the confinement potential and can be treated as a measure of the size of the QD. The potential-energy profile depicted in Fig. 6(a) corresponds to the QD studied by Ashoori *et al.*[3] In Sec. II, we have applied this potential energy to reproduce the capacitance-spectroscopy data.[3] At $V_g=-0.375$ V, the first electron is bound in the QD in the atomiclike state. Figure 6(a) shows that the parabolic approximation of the confinement potential energy is valid only for $r<100$ nm. In the large part of the QD located farther from the center, the confinement potential considerably deviates from the parabolic shape. If the cap radius increases, the lateral confinement potential energy becomes more flat near the QD center and more steep at the QD boundary. Figure 6(b) shows that for $R=800$ nm the confinement potential energy starts to resemble the rectangular potential well. This profile of the lateral confinement potential can be obtained using power-exponential formula (5) with large values of $p$ and $L$. Due to the flatness of the confinement potential the electrons localized in the QD are sensitive to the fluctuating potential created by the ionized donors in the barrier layer. In the presence of this fluctuating potential, the confined electrons do not form a well-defined atomiclike shell structure, which can explain a bunching observed in the addition spectra.[34] For small $R$ [cf. Fig. 6(c)] the confinement potential can be very well fitted over the entire nanodevice by the Gaussian potential well. The properties of one- and two-electron artificial atoms with the Gaussian confinement have been studied in Ref. 11.

The present modeling allows us to obtain the confinement potential, which exhibits the best parabolicity in the large region of the QD [Fig. 6(d)]. We have optimized the cap radius in order to obtain the parabolic confinement potential in as wide as possible a region of the nanodevice. We have found that for $R=120$ nm the confinement potential energy possesses the nearly ideal parabolic shape over almost entire region of the physical QD [cf. Fig. 6(d)].

All the profiles [Fig. 6(a)–6(d)] of the lateral confinement potential have been calculated under the assumption that exactly one electron forms the bound state in the QD. This assumption is fulfilled for the following gate voltages: $V_g=-0.375,-0.470,+0.100$, and $-0.125$ V for Figs. 6(a), 6(b), 6(c), and 6(d), respectively. We note that the values of both characteristic lengths, i.e., $R$ (cap radius) and $L$ (range of the model confinement potential), are very close to each other in the QD's considered [cf. Figs. 6(a)–6(d)]. Since $L$ provides a direct measure of the physical size of the QD, this agreement means that cap radius $R$ itself gives an accurate estimate of the spatial extension of the QD.

### B. Optimization of nanodevice parameters

In Sec. II we have shown that the present model of the electrostatic QD allows us to reproduce the experimental data of Ashoori *et al.*[2,3] In this section we apply this model to obtain the relevant physical quantities, which determine the electronic properties of the nanodevice.

Figures 5 and 6 show that the lateral confinement potential can be approximated quite well by the parabolic function

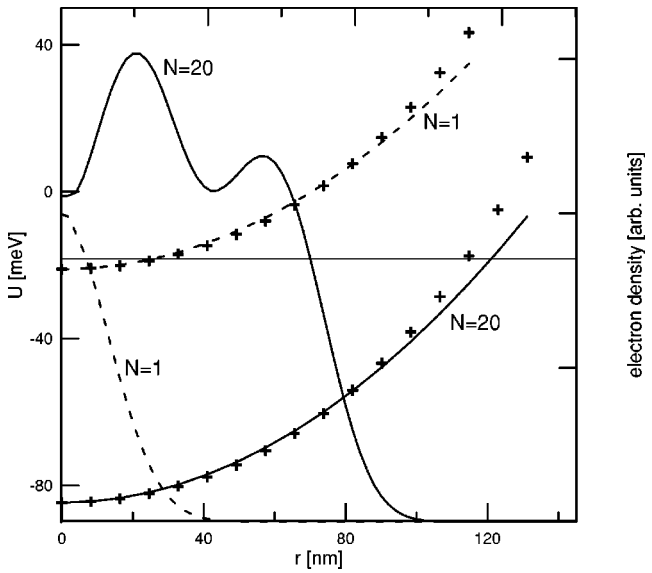


FIG. 7. Lateral confinement potential energy $U(r,z_0)$ (left scale) as a function of $r$ for $N=1$ and $N=20$ electrons confined in the QD. Numerical solutions of the Poisson equation are depicted by crosses and the parabolic fits by solid and dashed curves. The corresponding electron charge density calculated for $N=1$ and $N=20$ is drawn by the solid and dashed lines (right scale). The thin horizontal line corresponds to the Fermi energy decreased by the one-electron ground-state energy of the space-quantized motion in the $z$ direction.

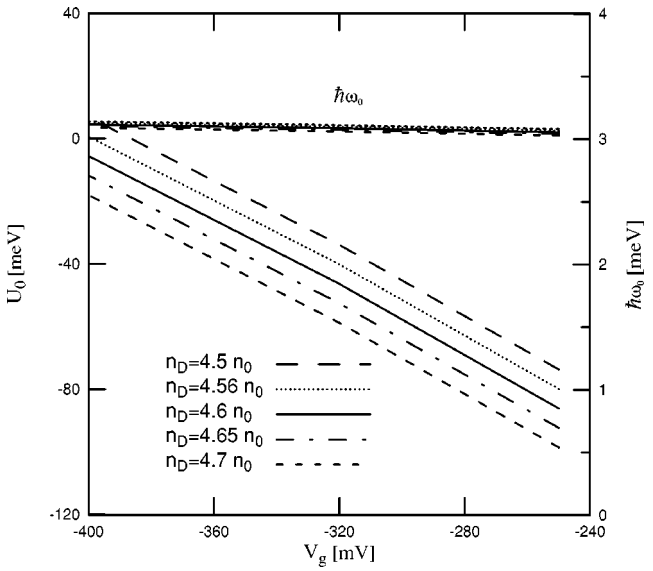


FIG. 8. Electron confinement potential-energy minimum $U_0$ (left scale) and confinement energy $\hbar\omega_0$ (right scale) as functions of gate voltage $V_g$ for several values of donor concentration $n_D$, where $n_0=10^{17}\,\mathrm{cm}^{-3}$.

if the dot radius is not too large. Therefore, the electronic properties of many QD's can be fairly well described using the parabolic confinement potential. Having at disposal the QD with a nearly parabolic confinement is very desirable due to a possibility of a simple prediction of its electronic properties. We can estimate how good is the approximate parabolicity of the confinement potential if we plot the confined charge-density distribution together with the realistic confinement potential profile as functions of distance $r$ from the cylinder axis. This comparison is depicted in Fig. 7 for $V_g=-0.375$ V for $N=1$ and $V_g=-0.292$ V for $N=20$. The electron charge density has been calculated by the Hartree-Fock method.[21] In Fig. 7 the crosses correspond to the numerical solutions of Poisson equation (3) and the solid and dashed curves show the parabolic approximations of these solutions. We see that the confinement potential is parabolic within the region of the electron localization. The electrons only slightly penetrate the nonparabolic region of the confinement potential. We note that the similar behavior was found[21] in the three-electrode QD of Tarucha *et al.*[5]

Let us consider the parabolic approximation of the lateral confinement potential energy

$$\tilde{U}(r)=U_0+\frac{m_e\omega_0^2}{2}r^2. \tag{6}$$

Potential energy (6) is characterized by the two parameters: $U_0$, i.e., the position of the potential-well minimum, and $\omega_0$, which determines the shape of the confinement potential energy near the minimum. The quantum of the oscillator energy, i.e., $\hbar\omega_0$, can be interpreted as the excitation energy and is usually called the confinement energy. Quantities $U_0$ and $\hbar\omega_0$ determine the electronic properties of the parabolic QD. We will show how these quantities depend on the parameters of the nanodevice, i.e., gate voltage $V_g$, number $N$ of electrons confined within the QD, concentration $n_D$ of the ionized donors, and radius $R$ of the cap.

The dependence of $U_0$ and $\hbar\omega_0$ on the gate voltage is displayed in Fig. 8. The confinement energy—with a good approximation—can be treated as a constant at different gate voltages. Potential-well bottom $U_0$ falls down almost linearly with increasing $V_g$, which means that the gate-voltage-to-energy conversion factor is approximately constant and equal to $\sim 0.5e$ (cf. Fig. 8). We note that the two-electrode QD, considered in the present paper, exhibits a different dependence on the gate voltage from the three-electrode vertical QD.[5] In the QD's of Tarucha *et al.*,[5] due to its more complex geometry, the confinement energy strongly depends on the gate voltage and changes in the interval 6.7 meV $\geqslant\hbar\omega_0\geqslant$5.4 meV if $N$ increases from 1 to 4. Moreover, the position of potential-well bottom $U_0$ is a nonlinear function of $V_g$.[21] As a result, the gate-voltage-to-energy conversion factor is a nonlinear function of $V_g$ and $N$.[21] The near independence of the conversion factor on $V_g$ in the two-electrode QD (Ref. 3) results from its simple, plane-capacitor-like structure. Figure 8 also shows that the increase of doping leads to the parallel downward shift of the linear functions $U_0(V_g)$.

Quantities $U_0$ and $\hbar\omega_0$ vary nearly linearly with number $N$ of electrons confined in the QD (Fig. 9). The position on the potential-well bottom $U_0$ decreases with increasing $N$ and confinement energy $\hbar\omega_0$ slowly increases with increasing $N$. The confinement energy can be treated as almost independent of $N$. The dependence of $U_0$ on the number of the QD confined electrons shows an important physical property

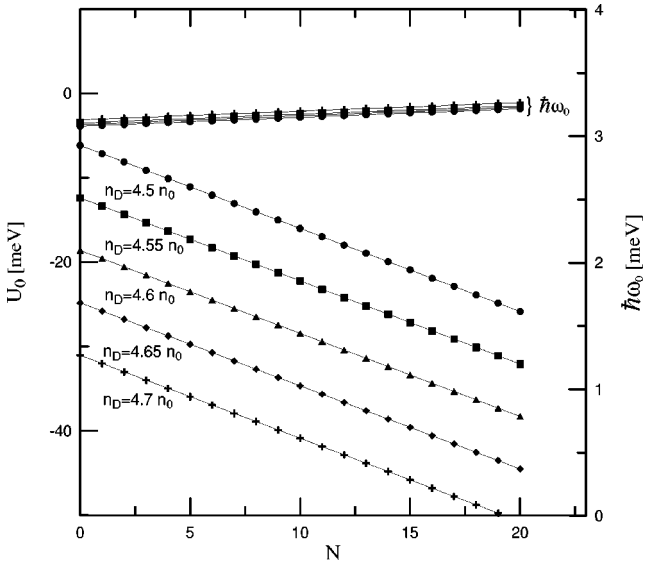


FIG. 9. $U_0$ (left scale) and $\hbar\omega_0$ (right scale) as functions of number $N$ of electrons confined in the QD for several values of donor concentration $n_D$, where $n_0=10^{17}$ cm$^{-3}$.

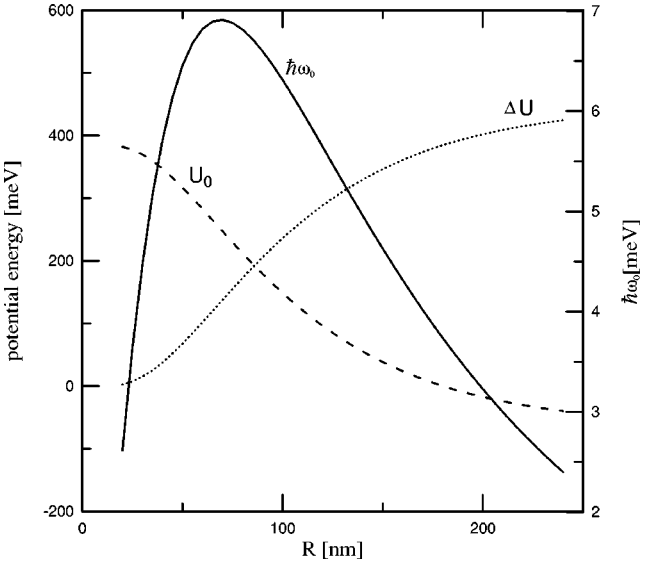


FIG. 11. Electron confinement potential-energy minimum $U_0$, lateral confinement potential well depth $\Delta U$ (left scale), and confinement energy $\hbar\omega_0$ (right scale) as functions of cap radius $R$ for fixed $n_D=4.62\times10^{17}$ cm$^{-3}$ and $V_g=-0.375$ meV.

of the nanodevice. This dependence results from the change of the induced charge distribution on the leads, which is caused by the presence of electrons in the QD. This effect considerably affects the electronic properties of the QD, but cannot be determined experimentally in a direct way.

Figure 10 shows the dependence of $U_0$ and $\hbar\omega_0$ on the concentration $n_D$ of the ionized donors for the three values of the cap radius. The donor concentration regime considered in Fig. 10 corresponds to the values of $U_0$ centered around zero. We have found that—in this donor concentration regime—confinement energy $\hbar\omega_0$ is almost independent of $n_D$ and potential-well bottom $U_0$ falls down approximately linearly with increasing $n_D$. The linear dependence of $U_0$ and $\hbar\omega_0$ on the ionized donor concentration is a rather unexpected behavior.

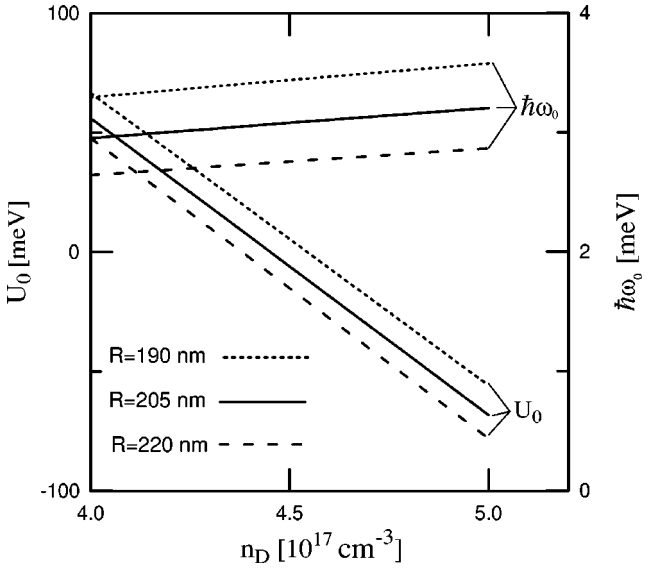


FIG. 10. $U_0$ (left scale) and $\hbar\omega_0$ (right scale) as functions of concentration $n_D$ of the ionized donors for three values of cap radius $R$.

Contrary to the linear dependencies shown in Figs. 8–10, the dependencies of both $U_0$ and $\hbar\omega_0$ on cap radius $R$ are highly nonlinear (Fig. 11). Potential-well minimum $U_0$ quickly falls down with $R$. Confinement energy $\hbar\omega_0$ is a nonmonotonic function of $R$. It increases with increasing $R$ for $R\leqslant65$ nm, takes on the maximum at $R=65$ nm, and next decreases with $R$. It is interesting that the maximal value of $\hbar\omega_0\simeq7$ meV corresponds to the nearly ideal Gaussian shape of the lateral confinement potential [cf. Fig. 6(c)]. Figure 11 also shows quantity $\Delta U$ (cf. Fig. 1), which is defined as $\Delta U=U(R_c,z_b)-U(0,z_b)$, where $R_c$ is the radius of the cylindrical surface, on which we put the boundary conditions, and $z_b$ is taken at the edge of the quantum well. $\Delta U$ can be interpreted as the depth of the lateral confinement potential well and is responsible for the lateral confinement of the electrons. This lateral confinement depth is a monotonically increasing function of $R$.

## IV. DISCUSSION

Let us compare the basic properties of the two types of the electrostatic QD's, namely, the two-electrode QD of Ashoori *et al.*[2,3] and the three-electrode QD of Tarucha *et al.*[5] In the electrostatic QD's the confinement potential depends on several parameters. The most important of them are the following: the geometry and composition of the nanodevice, the voltages applied to the electrodes, the spatial distribution of ionized impurities, and the charge confined in the QD. Since the dependence of the confinement potential on the structure of the nanodevice and the external electric field is rather well recognized, we shall concentrate on the effect of the ionized donor distribution and the electrons confined in the QD.

The total confinement potential energy [Eq. (1)] is strongly dependent on the charge, i.e., number of electrons, confined in the QD (cf. Figs. 5 and 9). The electrons confined within the QD create the electric field, which induces the charge on the leads, which in turn changes the net electrostatic field in the nanodevice. Therefore, we deal with the induced-charge effect, which can be taken into account either by the image charge method[13] or by separating both potentials [cf. Eq. (1)] and putting the proper boundary conditions on the total potential.[20,21]

The confinement potential in electrostatic QD's was calculated in few papers.[16,17,19–21] Bruce and Maksym[19] considered the three-electron Poisson-Schrödinger problem for the QD with the structure similar to that of Ashoori *et al.*[2,3] but built on the basis of slightly different layer sequence. In the present model and in the nanodevice of Ashoori *et al.*,[2,3] the electrons are localized in the $z$ direction in the GaAs potential well, which is separated from the substrate by the GaAs spacer and AlGaAs tunnel barrier. The model introduced by Bruce and Maksym[19] does not contain the potential well, but the electrons are bound in the inversion layer close to the interface of the AlGaAs barrier. The authors[19] included the interaction with the charge induced on the leads by the Green-function method.

The confinement potential in the three-electrode QD[5] was calculated by Matagne *et al.*[16,17] The calculated addition energies for $N=1,\ldots,20$ were compared[17] with the experimental data[5] and the qualitative agreement was obtained for the first seven addition energies. The lack of the quantitative agreement can be explained by the neglect of the redistribution of the ionized donors in the nanodevice. The authors[16,17] assumed the uniform distribution of the ionized donors in the entire doped region. In fact, the distribution of the ionized donors depends on both coordinates $r$ and $z$ and moreover changes with the voltages applied to the nanodevice and the charge confined in the QD, which in turn considerably modifies the confinement potential.[20,21] For the three-electrode QD the good quantitative agreement of the outcome of the calculations[20,21] with experiment[5] results from taking into account all the effects of crucial importance in this nanodevice.

The Poisson-Schrödinger problem for the three-electrode electrostatic QD[5] was solved in Refs. 20 and 21 with the help of a self-consistent procedure. The application of the self-consistent calculation scheme was necessary, since in the vertical gated QD[5] the spatial distribution of the ionized donors was unknown. This distribution, determined by the self-consistent procedure,[21] turned out to be a complicated function of coordinates, gate voltage, and number of electrons confined in the QD.[21] In the two-electrode electrostatic QD,[3] studied in the present paper, the spatial distribution of the ionized donors is homogeneous in the barrier layer. In the heavily doped substrate layer all the donors are entirely ionized in the thin layer close to the spacer, which is in contrast to the three-terminal nanodevice,[5] in which the ionized-donor region penetrates deeply into $n$-doped layers.[21] In the present simulation of the two-electrode QD the spatial distribution of the ionized donors in the thin, heavily doped, substrate layer close to the spacer is nonhomogeneous and is taken into account by the quickly convergent self-consistent scheme for solving Poisson equation (3).

The present results indicate that in the two-terminal QD nanodevice[3] the gate-voltage-to-energy conversion factor is constant, which results from the simple, plane-capacitor-like geometry of the device. In the QD of Tarucha *et al.*[5] this factor is a nonlinear function of the gate voltage, which is due to more complex geometry (circular gate surrounding the QD layer) and the strong dependence of the volume occupied by the ionized impurities and the lateral confinement energy on the gate voltage. In both types of the electrostatic QD's,[3,5] the bottom of the confinement potential is lowered when an additional electron enters the dot, which is due to the interaction between the confined charge and the charge induced outside the dot (in electrodes and $n$-GaAs layers). This effect, obtained in the present paper and in Ref. 21 from the solution of the Poisson equation, can also be qualitatively derived from the consideration of the image charges.[13]

We note that there is a striking difference between the two-[3] and three-terminal QD nanodevices[5] in the confinement potential dependence on the number of electrons confined within the QD. In both nanostructures,[3,5] number $N$ of confined electrons is controlled by the gate voltage, which, however, in the three-electrode QD of Tarucha *et al.*,[5] is applied to the third electrode placed on the side of the vertically etched pillar. Therefore, in the three-electrode QD,[5] the gate voltage has a pronounced influence on the shape of the confinement potential. In particular, the confinement potential gets flatter when the gate voltage increases, i.e., becomes less negative.[21] As a consequence the average electron density in the QD[5] is nearly independent of the number of confined electrons (cf. Fig. 4 in Ref. 21). Koskinen[35] derived the approximate expression for the dependence $\omega_0(N)$ assuming that the confined charge density is constant. According to this expression[35] the lateral confinement frequency decreases with the number of QD-confined electrons as $\hbar\omega_0 \sim N^{-1/4}$. The application[36] of this formula[35] leads to a qualitative agreement between the calculations[36] and the measured data.[5] However, the approximate formula[35] has a rather limited application and the qualitative description[36] of the QD of Tarucha *et al.*[5] seems to be accidental. In the QD of Ashoori *et al.*[3], the $\omega_0(N)$ dependence possesses a different character, namely, the lateral confinement energy slowly grows as $\hbar\omega_0 \sim N$ (cf. Fig. 9). In consequence, the average confined charge density is not independent of $N$, but also grows if the number of confined electrons increases (cf. Fig. 7). We note that the slow growth of the lateral confinement energy with $N$, obtained in the present paper (Fig. 9), is in qualitative agreement with the conclusions of Hawrylak,[13] drawn on the basis of the image charge approach.

## V. CONCLUSIONS

In the two-electrode electrostatic QD, studied in the present paper, the potential confining the electrons depends on the gate voltage, the donor concentration, the number of electrons confined in the QD, and the cap radius. We have determined these dependencies from the numerical solutions of the Poisson equation in the entire nanodevice. We have shown the ways of modeling the confinement potential pro-

file, which in turn leads to the required electronic properties of the nanodevice. In particular, we have studied the change of shape of the lateral confinement potential from the flat bottom, almost rectangular, potential well to the Gaussian potential well with smooth boundaries. The power-exponential formula[12] appears to be flexible enough to adjust all these potential profiles. We have found that the radius of the GaAs cap is a very important parameter that determines the shape of the confinement potential. The present calculations have been verified by a good agreement with the experimental data. The properties of the two-electrode QD of Ashoori *et al.*[3] have been compared with those of the three-electrode QD of Tarucha *et al.*,[5] and the similarities and differences of both nanodevices have been discussed in detail.

In summary, the following effects are found to be of crucial importance when determining the electronic properties of the electrostatic QD's: the composition and geometry of the nanodevice, the gate voltage, the distribution of the ionized impurities, and the charge induced on the leads by the charge confined in the QD. We have shown that the model, which properly takes into account all these effects, leads to a good quantitative agreement with the experiment.

## ACKNOWLEDGMENT

This work was supported in part by the Polish Government Scientific Research Committee (KBN).

*Email address: adamowski@ftj.agh.edu.pl.

[1] P.A. Maksym and T. Chakraborty, Phys. Rev. Lett. **65**, 108 (1990).
[2] R.C. Ashoori, H.L. Stormer, J.S. Weiner, L.N. Pfeiffer, S.J. Pearton, K.W. Baldwin, and K.W. West, Phys. Rev. Lett. **68**, 3088 (1992).
[3] R.C. Ashoori, H.L. Stormer, J.S. Weiner, L.N. Pfeiffer, K.W. Baldwin, and K.W. West, Phys. Rev. Lett. **71**, 613 (1993); Physica B **189**, 117 (1993).
[4] R.C. Ashoori, N.B. Zhitenev, L.N. Pfeiffer, and K.W. West, Physica E (Amsterdam) **3**, 15 (1998).
[5] S. Tarucha, D.G. Austing, T. Honda, R.J. van der Hage, and L.P. Kouwenhoven, Phys. Rev. Lett. **77**, 3613 (1996).
[6] S.R.E. Yang, A.H. MacDonald, and M.D. Johnson, Phys. Rev. Lett. **71**, 3194 (1993).
[7] D. Pfannkuche, V. Gudmundsson, and P.A. Maksym, Phys. Rev. B **47**, 2244 (1993).
[8] N.F. Johnson, J. Phys.: Condens. Matter **7**, 965 (1995).
[9] O. Steffens, U. Rössler, and M. Suhrke, Europhys. Lett. **43**, 529 (1998).
[10] F.M. Peeters and V.A. Schweigert, Phys. Rev. B **53**, 1468 (1996).
[11] J. Adamowski, M. Sobkowicz, B. Szafran, and S. Bednarek, Phys. Rev. B **62**, 4234 (2000).
[12] M. Ciurla, J. Adamowski, B. Szafran, and S. Bednarek, Physica E (Amsterdam) **15**, 261 (2002).
[13] P. Hawrylak, Phys. Rev. Lett. **71**, 3347 (1993).
[14] L. Jacak, P. Hawrylak, and A. Wójs, *Quantum Dots* (Springer, Berlin, 1998).
[15] S.M. Reimann, M. Koskinen, M. Manninen, and B.R. Mottelson, Phys. Rev. Lett. **83**, 3270 (1999).
[16] P. Matagne, J.P. Leburton, D.G. Austing, and S. Tarucha, Phys. Rev. B **65**, 085325 (2002).
[17] P. Matagne and J.-P. Leburton, Phys. Rev. B **65**, 235323 (2002).
[18] M. Grundmann, O. Stier, and D. Bimberg, Phys. Rev. B **52**, 11 969 (1995).
[19] N.A. Bruce and P.A. Maksym, Phys. Rev. B **61**, 4718 (2000).
[20] S. Bednarek, B. Szafran, and J. Adamowski, Phys. Rev. B **61**, 4461 (2000).
[21] S. Bednarek, B. Szafran, and J. Adamowski, Phys. Rev. B **64**, 195303 (2001).
[22] L.P. Kouwenhoven, T.H. Oosterkamp, M.W.S. Danoesastro, M. Eto, D.G. Austing, T. Honda, and S. Tarucha, Science **278**, 1788 (1997).
[23] N.B. Zhitenev, M. Brodsky, R.C. Ashoori, L.N. Pfeiffer, and K.W. West, Science **285**, 715 (1999).
[24] M. Brodsky, N.B. Zhitenev, R.C. Ashoori, L.N. Pfeiffer, and K.W. West, Phys. Rev. Lett. **85**, 2356 (2000).
[25] S. Sasaki, S. De Franchesci, J.M. Elzerman, W.G. van der Wiel, M. Eto, S. Tarucha, and L.P. Kouwenhoven, Nature (London) **405**, 764 (2000).
[26] K. Lis, S. Bednarek, B. Szafran, and J. Adamowski, Physica E **17**C, 494 (2003).
[27] N.B. Zhitenev, R.C. Ashoori, L.N. Pfeiffer, and K.W. West, Phys. Rev. Lett. **79**, 2308 (1997).
[28] R.J. Luyken, A Lorke, M. Haslinger, B.T. Miller, M. Fricke, J.P. Kotthaus, G. Medeiros-Ribeiro, and P.M. Petroff, Physica E (Amsterdam) **2**, 704 (1998).
[29] M. Brodsky, Ph.D. thesis, MIT, 2000, See http://electron.mit.edu/theses/misha_thesis.pdf
[30] R. Kosloff and H. Tal-Ezer, Chem. Phys. Lett. **127**, 223 (1986).
[31] B. Szafran, S. Bednarek, and J. Adamowski, Phys. Rev. B **67**, 115323 (2003).
[32] M. Wagner, U. Merkt, and A.V. Chaplik, Phys. Rev. B **45**, 1951 (1992).
[33] B. Szafran, S. Bednarek, and J. Adamowski, Phys. Rev. B **65**, 035316 (2002); **66**, 199903(E) (2002).
[34] C.M. Canali, Phys. Rev. Lett. **84**, 3934 (2000).
[35] M. Koskinen, M. Manninen, and S.M. Reimann, Phys. Rev. Lett. **79**, 1389 (1997).
[36] S.M. Reimann, M. Koskinen, M. Manninen, and B.R. Mottelson, Phys. Rev. Lett. **83**, 3270 (1999).